



Cysteine-based chiral selectors for the ligand-exchange separation of amino acids[☆]

Benedetto Natalini^{*}, Roccaldo Sardella, Antonio Macchiarulo, Roberto Pellicciari

Dipartimento di Chimica e Tecnologia del Farmaco, Università degli Studi di Perugia, Via del Liceo 1, 06123 Perugia, Italy

ARTICLE INFO

Article history:

Received 28 March 2008

Accepted 3 June 2008

Available online 11 June 2008

Keywords:

Chiral ligand-exchange chromatography

Enantiomer separation

Molecular descriptors

Classification system

Chiral coated phase

ABSTRACT

Three cysteine-based coated selectors, S-benzyl-(R)-cysteine, S-diphenylmethyl-(R)-cysteine and S-trityl-(R)-cysteine, have been used in the ligand-exchange separation of a selected set of natural and unnatural underivatized amino acids. With only few exceptions, a gain in enantiodiscrimination was obtained when the most lipophilic discriminating agent, characterized by the presence of a trityl moiety, was engaged. Moreover, a new descriptive structure–separation relationship study through molecular surface (Jurs) and shape (Shadow) descriptors provided evidence that specific physico-chemical features of the employed chiral selector result decisive in establishing which property of the analyte is responsible for the enantio-recognition accomplishment.

© 2008 Elsevier B.V. All rights reserved.

1. Introduction

Glutamate receptor modulators are retained of utmost importance in the pharmacological control of major central nervous system (CNS) disorders. Independent yet converging research efforts claim for a crucial involvement of Glu receptors in the mechanism of action of antidepressant [1], antipsychotic [2], antiparkinsonian [3,4] and nociceptive processing [5] drugs. Our continuing interest in this very challenging and promising field of research led us to develop potent and selective ligands for the various members of both ionotropic and metabotropic glutamate receptor families [6–13]. All the synthesized amino acidic compounds have been analyzed through chiral ligand-exchange chromatography (CLEC) in order to assess the optical purity and, eventually, the enantiomeric excess. In some cases [11,14,15] we have also provided for the preparative separation of enantiomers through this technique: for example, 1-aminoindane-1,5-dicarboxylic acid (AIDA) enantiomers [14,15] have been successfully separated and tested for the first time.

Very recently [15] we have reported on the separation and resolution ability of S-trityl-(R)-cysteine [(R)-STC] (Fig. 1), a new,

dynamically coated chiral selector which proved to be very effective in both analytical and preparative-scale separation of some natural and unnatural underivatized amino acid enantiomers. We also described the influence of the side chain lipophilic moiety constituted by an aromatic portion and a sulphur atom as a spacer endowed with additional hydrophobic character [15]. A comparison between (R)-STC and S-benzyl-(R)-cysteine [(R)-SBC] (Fig. 1), which differ for the number of the aromatic rings in the side chain, has been also performed with the aim of identifying molecular properties of analytes that affect the enantiodiscrimination process through a descriptive structure–separation relationship (DSSR) study [16]. For such a purpose, the selection was directed toward a cumulative pool of 40 descriptors (Jurs [17] and Shadow descriptors [18]) which relate to the physico-chemical properties and shape of the molecular surface area.

A wide variety of QSPR strategies based on the extra-thermodynamic approach and including linear solvation energy relationship (LSER) studies [19], 3D-QSPR comparative molecular field analysis (CoMFA) [20], linear free energy relationship (LFER) studies [21–23], and comparative molecular similarity index analysis (CoMSIA) methods [24], have been engaged for getting a deeper insight into the enantioselective process in HPLC. However, no application has been directed to CLEC with this regard.

For the first time we proposed a new classification strategy aimed at casting a new light on the mechanism that rules the enantiodifferentiation in CLEC. Oppositely to the most common computational treatments, no multiple linear regression analysis (MLRA) has been here performed. The key contribution from our

[☆] This paper is part of the Special Issue 'Enantioseparations', dedicated to W. Lindner, edited by B. Chankvetadze and E. Francotte.

^{*} Corresponding author. Tel.: +39 075 5855131; fax: +39 075 5855161.

E-mail address: natalini@chimfarm.unipg.it (B. Natalini).

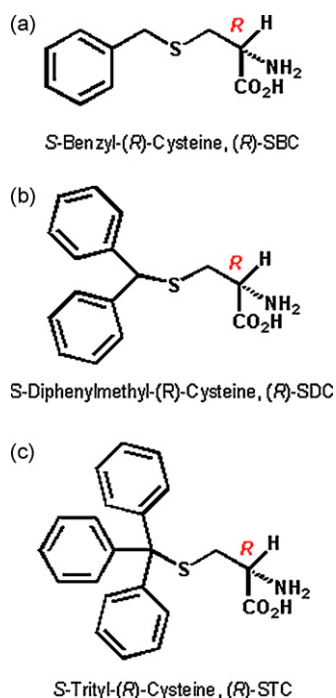


Fig. 1. Chiral selectors investigated in this study: (a) S-benzyl-(*R*)-cysteine [(*R*)-SBC]; (b) S-diphenylmethyl-(*R*)-cysteine [(*R*)-SDC]; (c) S-trityl-(*R*)-cysteine [(*R*)-STC].

methodology deals with the possibility to establish the actual enantiodiscrimination capability exerted by a selected discriminating agent toward a specific analyte. This procedure wants to make easier the proper selection of the discriminating agent especially in the case of small available amounts of the analyte.

The relevant effectiveness of such an approach in establishing molecular properties responsible for the enantio-recognition accomplishment prompted us to further assess its validity. Accordingly, in order to fully cover the lipophilic scenario of the cited aromatic ring containing cysteine selectors and hence to derive useful information on the mechanism of chiral recognition, the chromatographic performances afforded by the S-diphenylmethyl-(*R*)-cysteine [(*R*)-SDC] (Fig. 1) were then investigated. Here we report the results obtained with the new chiral selector as well as a comparison among the performances showed by the three sulfur-containing discriminating agents.

2. Experimental

2.1. Chemicals and standards

HPLC grade water was obtained from a tandem Milli-Ro/Milli-Q apparatus (Millipore, Bedford, MA, USA). The enantiomers of 1-aminoindane-1,5-dicarboxylic acid (AIDA) [7], 2-(5'-carboxy-thien-2'-yl)glycine (ATIDA) [25] and 2-(5'-methyl-4'-carboxythien-2'-yl)glycine (5-MATIDA) [25] were prepared in our laboratory. The enantiomers of the four compounds 3a,5,6,6a-tetrahydro-4*H*-pyrrolo[3,4-*d*]isoxazole-3,4-dicarboxylic acid (CIP-A), 3a,5,6,6a-tetrahydro-4*H*-pyrrolo[3,4-*d*]isoxazole-3,6-dicarboxylic acid (CIP-B), 5-(2-amino-2-carboxyethyl)-4,5-dihydroisoxazole-3-carboxylic acids (F94B and F94C) were kindly provided by De Amici and co-workers [26]. All the remaining amino acid enantiomers, the three chiral selectors and the copper(II) sulphate pentahydrate were of high analytical purity and purchased from Sigma–Aldrich (Milan, Italy). Mobile phases solu-

tions were filtered through a 0.45 μ m Millipore filter and degassed with 10 min sonication before use. All samples were prepared in approximate concentrations between 0.1 and 0.5 mg/mL in filtered mobile phase components and sonicated until completely dissolved.

2.2. Instrumentation

The HPLC analytical-scale experiments were carried out on a Shimadzu (Kyoto, Japan) LC-Workstation Class LC-10 equipped with a CBM-10A system controller, two LC-10AD high pressure binary gradient delivery systems, a SPD-10A variable-wavelength UV–vis detector and a Rheodyne 7725i injector (Rheodyne, Cotati, CA, USA) with a 20 μ L stainless steel loop.

2.3. Dynamic coating and column evaluation

Analytical scale runs were made on a LiChrospher 100 RP-18 (Merck, 250 mm \times 4 mm i.d., 5 μ m, 100 Å) analytical column coated with the employed chiral selector, by recycling a methanol–water solution (250 mL, 75:25, v/v) of the chiral discriminating agent (0.1 g) for 5 days at 0.5 mL/min. Before recycling, the chiral selector solution was carefully filtered through a 0.45 μ m Millipore filter and degassed with 10 min sonication. Changes in the absorbance of the eluent were followed by UV detection at 254 and 210 nm. Equilibrium in the coating process was indicated by an initial abrupt rise in the UV baseline which then progressively stabilizes to the new baseline condition. With this procedure, an approximated amount of 0.068 g of (*R*)-SBC, 0.057 g of (*R*)-SDC and 0.045 g of (*R*)-STC were hydrophobically bound to the RP-18 sorbent surface. These amounts almost linearly oppose the bulkiness of the selector side chain, thus showing a different hydrophobic coating of the reversed-phase material [27].

After washing with a water–methanol solution (50 mL, 98:2, v/v) in order to displace the excess of chiral discriminating agent and methanol, the copper(II) sulphate solution was used as the mobile phase. After 2 h of equilibration, NaNO₂ injection peak was used for a completely unretained marker in all analyses. Column performance was assayed with periodical injection of *rac*-Pro. The dynamic CSPs from (*R*)-SBC, (*R*)-SDC and (*R*)-STC were found to be stable and equally effective for chiral separation of amino acids for at least 5, 20 and 30 days, respectively.

2.4. System precision

The short-term repeatability is the relative standard deviation (RSD) of the results of three consecutive runs carried out with one column over a period of few hours [28]. We report the short-term repeatability data for both retention (*k*) and separation (α) factors measured when the (*R*)-SDC was used as the chiral discriminating agent.

2.5. Molecular modeling methods

A training set containing 32 compounds and a validation set of 8 compounds were collected with the relative experimental separation factor α . The training set consists in compounds with an input vector of molecular descriptors and an answer vector of experimental α values that are used to train a statistical model of DSSR. The validation set consists of compounds with only an input vector of molecular descriptors whose experimental α values are used to validate the predictive reliability of the statistical model.

The compounds belonging to the training set were assigned to two classes on the basis of their α value. While class 1 comprised all

the undiscriminated enantiomer couples (namely those characterized by $\alpha = 1$), class 2 included all the separated ones (namely, those with $\alpha > 1$). Structural models of all compounds were constructed starting from the fragment dictionary of Cerius-2 (Accelrys, San Diego, CA) in their neutral form (formal charge = 0) and the resulting geometry was optimized using the semiempirical MOPAC/AM1 method. Atomic charges were computed using the electrostatic potential fitting approach (ESP charges). For each compound, a pool of 30 molecular surface area descriptors (Jurs-descriptors [17]) and 10 shape descriptors (Shadow-descriptors [18]) were calculated using the descriptor module implemented in Cerius-2. While Jurs capture the shape and electronic information of the molecules by mapping atomic partial charges on solvent-accessible surface areas of individual atoms, Shadow descriptors encode the geometric arrangement of the molecular shape of the molecules by aligning the principal moments of inertia with the X, Y, and Z axes and then projecting the molecular surface on the three mutually perpendicular planes (XY, YZ, and XZ). Since both Jurs and Shadow descriptors depend on the configuration and conformation of the compounds, the global minimum conformer of all (R)- and (S)-isomers was used in the calculation. The classification study was carried out using the recursive partitioning method as implemented in Cerius-2. In particular, the following main settings were used. Classes were equally weighted, split scoring was performed using the Gini Impurity rule; a moderate pruning (=3) was performed; nodes should contain 1/100 of samples; the number of threshold values tested in order to make node splits on the independent variables (knot limit) was set to a value of 20; the maximum number of node splits that could yield to a terminal node (Maximum Tree Depth) was set to a value of 5.

3. Results and discussion

3.1. Comparison among the chromatographic performances obtained from the three investigated chiral coated phases

In order to rank the three compounds for their lipophilicity, and describe their side chain contribution to the solvent accessibility surface area, a calculation performed with the same software (Cerius-2) used for the classification study afforded the values reported in Table 1. Retention (k) and separation (α) factors obtained with the three sulfur-containing selectors for the amino acids selected as the training set have been reported in Table 2. The chromatographic behaviour observed with the three chiral selectors offered some interesting consideration. With all the adopted selectors, aspartic acid (Asp), F94C, O-phospho-serine (O-Pho-Ser) and ornithine (Orn) enantiomer couples did not experience any enantio-recognition. While a comparable enantioseparation of threonine (Thr) antipodes was achieved with (R)-STC and (R)-SDC, (R)-SBC was not effective thus providing for the enantiomers coelution [16]. With the exception of 5-MATIDA, F94B, cysteine (Cys) and CIP-B enantiomer couples which resulted better discriminated with (R)-SDC, a gain in enantiodiscrimination was obtained for all the remaining compounds when the most lipophilic chiral selector was engaged [(R)-STC]. As an example, the chromatograms of 3,4-dehydro-proline (3,4-DeHy-Pro) enantiomer couple with all the

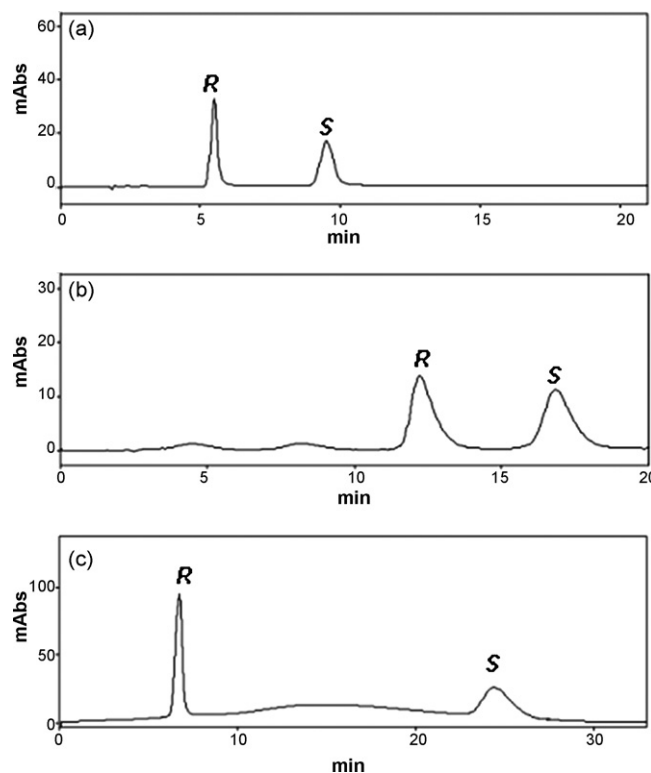


Fig. 2. Chromatograms of 3,4-dehydro-proline (3,4-DeHy-Pro) with: (a) (R)-SBC; (b) (R)-SDC; (c) (R)-STC. Experimental conditions: mobile phase, 1.0 mM Cu(II) sulphate; flow rate, 1.0 mL/min; injection volume, 20 μ L; UV at 254 nm; column temperature, 20 $^{\circ}$ C.

investigated chiral selectors are reported in Fig. 2. With reference to the two structural isomeric couples, isoleucine/leucine (Ile/Leu) and CIP-A/CIP-B, controversial results have been encountered. Indeed, while all the selectors afforded higher enantiodiscriminating ability for Ile over Leu enantiomers, a progressive inversion of the chromatographic performances interested CIP isomers, being the CIP-B couple better resolved with the chiral selector endowed with the intermediate lipophilicity [(R)-SDC]. Particularly intriguing is the chromatographic response for F94B and F94C enantiomer couples. Indeed, while all the selectors supplied enantioseparation for the former, the latter always resulted undiscriminated. This is evidently the case in which all the discriminating agents do not 'feel' the differences in the spatial configuration of the two enantiomers, thus showing their inability in discriminating between their orientation along the three axes [29]. Although the dynamic coating method, first proposed by Davankov in the early 1980s, [30] revealed to be successful for the resolution of enantiomer couples of suitable bi-chelating compounds, however, it turned out that heterogeneous surfaces are produced through the adsorption of an appropriate resolving agent onto the surface of a conventional reversed phase material. Consequently, all the generated chiral columns are endowed with two different types of adsorption sites. While those generally named of type-I deal with nonselective interactions (low-energy molecular interactions) the others known as type-II refer to all the enantioselective ones (high adsorption energy) [28–34].

Type-I principally embraces hydrophobic and dispersive interactions, however hydrogen bond interactions are encompassed as well. These interactions are responsible for retention on conventional achiral packings (e.g., with the alkyl chains as well as the underivatized silanols in a RP column). Both types of interactions are present on all CSPs regardless the specific mechanism gov-

Table 1
Selected physico-chemical parameters of the investigated chiral selectors

Chiral selector	A log P	Solvent-accessible area (\AA^2)
(R)-SBC	1.18	214.28
(R)-SDC	3.03	281.22
(R)-STC	4.54	335.75

A log P, atomic partition coefficient.

Table 2

Structures and selected chromatographic parameters for the training-set investigated in this study

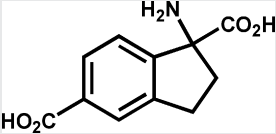
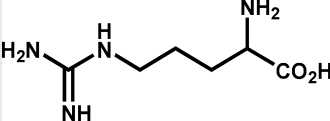
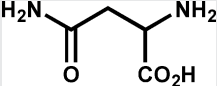
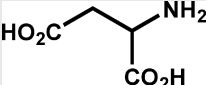
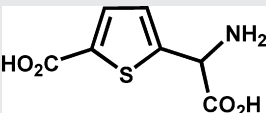
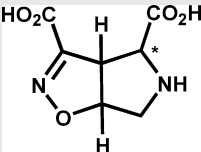
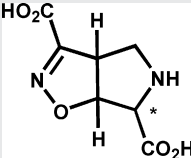
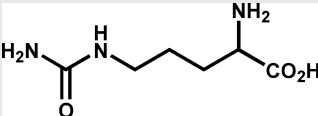
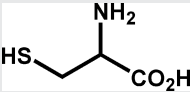
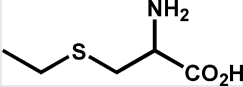
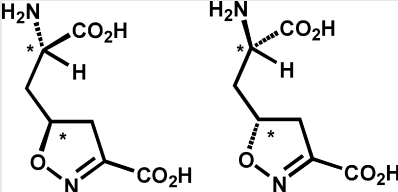
Sample	Structure	(R)-STC			(R)-SDC			(R)-SBC		
		k_R	k_S	α	k_R	k_S	α	k_R	k_S	α
AIDA		8.79	3.78	2.33	1.40	0.96	1.45	1.61	1.16	1.39
Arg		1.57	8.22	5.24	2.05	4.70	2.29	3.72	4.61	1.24
Asn		0.38	0.55	1.45	0.27	0.27	1.00	0.37	0.37	1.00
Asp		0.58	0.58	1.00	0.22	0.22	1.00	0.11	0.11	1.00
ATIDA		2.53	2.13	1.19	0.11	0.11	1.00	0.20	0.20	1.00
CIP-A		1.82	7.73	4.25	0.59	1.43	2.44	0.78	1.26	1.62
CIP-B		2.47	4.50	1.82	0.07	0.23	3.49	0.28	0.28	1.00
Cit		1.25	1.54	1.23	0.87	0.87	1.00	0.91	0.91	1.00
Cys		22.34	22.34	1.00	3.22	5.35	1.66	2.33	3.28	1.41
Eth		29.24	45.42	1.55	26.06	30.92	1.19	24.30	30.81	1.27
F94B		2.75	3.57	1.30	0.19	0.87	4.46	0.28	1.09	3.89

Table 2 (Continued)

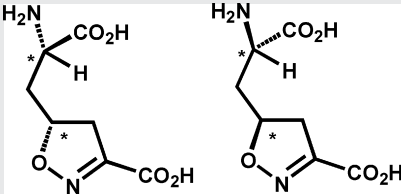
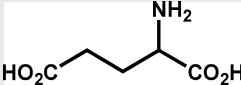
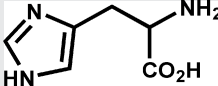
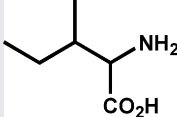
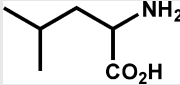
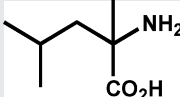
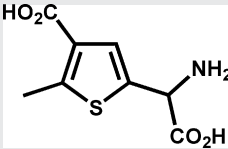
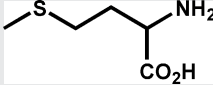
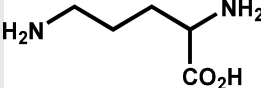
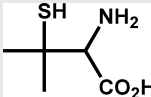
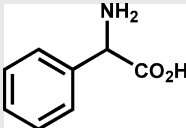
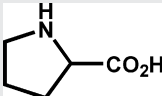
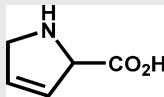
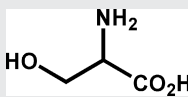
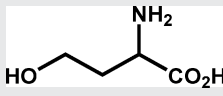
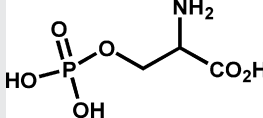
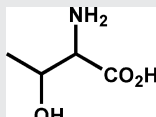
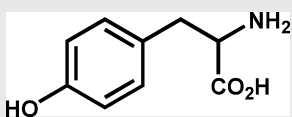
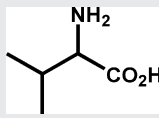
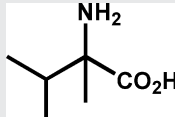
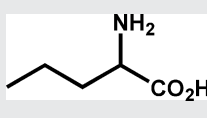
Sample	Structure	(R)-STC			(R)-SDC			(R)-SBC		
		<i>k_R</i>	<i>k_S</i>	α	<i>k_R</i>	<i>k_S</i>	α	<i>k_R</i>	<i>k_S</i>	α
F94C		2.56	2.56	1.00	0.41	0.41	1.00	0.25	0.25	1.00
Glu		0.76	0.92	1.21	0.36	0.36	1.00	0.21	0.21	1.00
His		4.26	3.16	1.35	1.91	1.68	1.14	2.00	1.55	1.29
Ile		10.75	22.80	2.12	11.11	19.28	1.73	11.64	18.21	1.56
Leu		11.01	17.04	1.55	14.95	19.18	1.28	12.60	16.47	1.31
α -Me-Leu		13.82	25.03	1.81	23.58	31.18	1.32	7.81	9.07	1.16
5-MATIDA		17.66	16.55	1.07	2.65	2.35	1.13	3.13	3.13	1.00
Met		9.21	13.33	1.45	6.77	8.16	1.20	6.59	8.03	1.22
Orn		0.14	0.14	1.00	0.46	0.46	1.00	0.57	0.57	1.00
Pen		2.70	3.82	1.41	0.48	0.48	1.00	0.80	0.80	1.00
Phg		9.81	17.38	1.77	9.03	12.16	1.35	7.67	11.54	1.50
Pro		1.79	9.32	5.21	2.11	4.95	2.34	1.77	4.23	2.39

Table 2 (Continued)

Sample	Structure	(R)-STC			(R)-SDC			(R)-SBC		
		k_R	k_S	α	k_R	k_S	α	k_R	k_S	α
3,4-DeHy-Pro		1.87	9.50	5.08	1.75	4.07	2.33	1.79	3.86	2.16
Ser		0.32	0.32	1.00	0.44	0.44	1.00	0.38	0.38	1.00
Homo-Ser		0.69	0.88	1.28	0.46	0.46	1.00	0.52	0.52	1.00
O-Pho-Ser		2.30	2.30	1.00	0.12	0.12	1.00	0.15	0.15	1.00
Thr		0.51	0.69	1.35	0.47	0.64	1.37	0.59	0.68	1.15
Tyr		13.44	26.22	1.95	15.02	15.69	1.05	15.03	16.42	1.09
Val		3.29	6.93	2.11	3.58	5.32	1.49	3.26	4.64	1.42
α -Me-Val		6.35	10.63	1.67	6.92	7.85	1.13	7.63	8.87	1.16
Nor-Val		3.84	6.53	1.70	4.46	5.94	1.33	3.76	4.95	1.32

Experimental conditions: mobile phase, 1.0 mM Cu(II) sulphate; flow rate, 1.0 mL/min; injection volume, 20 μ L; UV at 254 nm; column temperature, 20 °C.

erning the recognition process. Consequently, the retention factor can be considered as the sum of two contributions originating from type-I and type-II sites, respectively. Even in a CLEC environment, the capacity factor (k) depends on both analyte adsorption (either through an one- or two-step mechanism [34]) and complexation process. This generally implies that by increasing the ligand-exchange sorption sites concentration as well as the sorption power of the achiral support, an enhancement in terms of retention should be observed. However, although type-II sites are most plausibly less abundant than type-I, complex formation is the dominant factor controlling retention [30]. Both contributions can be tuned to a different extent depending on the adopted experimental conditions [30]. The ineffectiveness displayed by the (R)-STC based CSP in the discrimination of Cys enantiomers can be explained on this basis. Indeed, rather than an insufficient difference in the molar free energy of formation ($\Delta\Delta G$) between the two transient

diastereomeric ternary complexes, the occurrence of significant nonselective interactions appears to be actually more plausible. In other words, the contribution to the chromatographic enantioselectivity (α_{chrom}) exerted by nonselective interactions expressed with the a_1 factor in the following equation [31,33,34]:

$$\alpha_{\text{chrom}} = \frac{a_1 + a_{2,\text{II}}}{a_1 + a_{1,\text{II}}} \quad (1)$$

where a_1 refers to all the nonselective interactions and $a_{2,\text{II}}$ and $a_{1,\text{II}}$ correspond to the equilibrium constants of the interactions of the second and the first retained enantiomer on the type-II sites, is the prevalent one. Even if to a minor extent, tyrosine (Tyr) with both (R)-SBC and (R)-SDC and 5-MATIDA with (R)-STC experienced a similar behaviour. Although quite strongly retained, they did not undergo any decent enantioseparation. In principle, likewise all the other enantioselective chromatographic strategies,

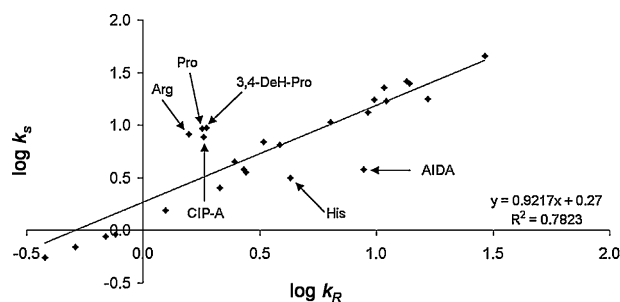


Fig. 3. Evidence of the diversity in their enantiomer-mixed chiral stationary phase association by Arg, CIP-A, Pro, 3,4-DeHy-Pro, AIDA and His samples, from the $\log k_S$ vs. $\log k_R$ plot. Experimental conditions: mobile phase, 1.0 mM Cu(II) sulphate; flow rate, 1.0 mL/min; injection volume, 20 μ L; UV at 254 nm; column temperature, 20 °C.

even in a CLEC environment, the chromatographic enantioselectivity can only approach that coming out from the pure solute-selector association (theoretical enantioselectivity) only if the nonselective affinity of the solute toward the stationary phase remains negligible [35]. Pure thermodynamic considerations can also be recalled for tentatively explaining the above scarce or completely missing enantioseparation. As well known, the enthalpic contribution to α_{chrom} generally prevails on the entropic one. Sometimes, however, noticeable differences in the entropy of diastereomers formation render this contribution comparable, or even exceeding, the enthalpic one. Consequently, the selector enantioselectivity capability results to be restrained. This circumstance mainly comes out when a different number of solvent molecules takes part to the transient complex formation [29]. With the most lipophilic chiral discriminating agent [(R)-STC], arginine (Arg), CIP-A, proline (Pro) and 3,4-DeHy-Pro represent extraordinary examples of the so-called 'kinetic enantioselectivity' (Table 2). Indeed, for all these couples, besides the observed four, five or even sixfold higher retention experienced by the second eluted peak, the first eluted one always accompanies with a relatively low retention. For Arg, CIP-A, Pro and 3,4-DeHy-Pro enantiomer couples, Fig. 3 unambiguously puts into evidence the diversity in their enantiomer-mixed chiral stationary phase association. While for CIP-A, Pro and 3,4-DeHy-Pro this difference can be demanded to their structural rigidity, the presence of a planar, guanidinic group in Arg can favour sticking interactions with the chiral selector aromatic portion which should noticeably stabilize the cisoid arrangement. Moreover, the inversion of elution order for AIDA and histidine (His) can be claimed for explaining their behaviour as two outlier in the same plot (Fig. 3). As a general principle, while the kinetic enantioselectivity is a measure of the difference in the association rate between the chiral selector and the two enantiomers, the most considered thermodynamic enantioselectivity entails with the difference in the intensity of the occurring interactions, i.e., the difference in the stability of the two transient diastereomeric complexes. Davankov [36] reported that there is no thermodynamic without kinetic enantioselectivity, whereas the opposite assertion is not valid. With all the employed sulphur-containing chiral selectors and with the exception of His and AIDA, (S)-enantiomers are more retained than their antipodes [16,37]. Thiophene-derived amino acids do not represent exceptions since the presence of the sulphur atom reverses the usual amino acid priority. On the basis of the obtained results, we have

Table 3

Relative standard deviation values for enantiomers retention (k) and separation (α) factors with the (R)-SDC as the chiral selector

Sample	RSD (%)			Sample	RSD (%)		
	k_R	k_S	α		k_R	k_S	α
AIDA	3.20	3.60	0.00	α -Me-Leu	3.11	3.46	0.76
Arg	3.25	3.12	0.67	5-MATIDA	3.98	3.90	0.00
Asn		Unresolved		Met	0.17	0.14	0.00
Asp		Unresolved		Orn		Unresolved	
ATIDA		Unresolved		Pen		Unresolved	
CIP-A	8.51	4.07	3.32	Phg	1.59	1.35	0.74
CiIP-B		Unresolved		Pro	3.73	3.24	0.79
Cit		Unresolved		3,4-DeHy-Pro	1.10	0.89	1.00
Cys	2.16	3.00	0.63	Ser		Unresolved	
Eth	3.54	1.03	4.88	Homo-Ser		Unresolved	
F94B	0.00	8.00	0.16	O-Pho-Ser		Unresolved	
F94C		Unresolved		Thr	0.00	2.08	0.60
Glu		Unresolved		Tyr	1.33	1.27	0.43
His	3.15	2.01	4.35	Val	3.11	3.46	0.76
Ile	2.15	3.18	0.37	α -Me-Val	1.16	0.38	0.00
Leu	2.64	2.03	0.79	Nor-Leu	5.50	4.99	0.74

Experimental conditions: mobile phase, 1.0 mM Cu(II) sulphate; flow rate, 1.0 mL/min; injection volume, 20 μ L; UV at 254 nm; column temperature, 20 °C.

already proposed a chiral recognition model showing the formation of the two energetically different diastereomeric ternary complexes with (R)-SBC as the chiral selector [37]. However, analogous considerations are still applicable with (R)-SDC and (R)-STC.

A generally high short-term repeatability is afforded by the three investigated chiral systems with respect to the selected chromatographic parameters (retention and enantioseparation factors). As an example, only the case of the enantioresolving agent endowed with the intermediate lipophilic character is examined. Accordingly, small variations of both enantioselectivity and capacity factors were observed when employing an RP-18 column coated with the (R)-SDC as the chiral discriminating agent. Indeed, the RSD values of the separation factors are in the range 0.0–4.9%, while concerning the retention factors these ranged between 0.0 and 8.5 for the (R)-enantiomers and between 0.1 and 5.0 for their antipodes [(S)-enantiomers] (Table 3).

3.2. Descriptive structure-separation relationship study

A partition tree or classification model analysis was performed on the training set of 32 analytes along with their experimental separation factors (α) calculated using (R)-SDC as the chiral selector in the mixed stationary phase. In the classification study, each compound of the training set was assigned to class 1 or class 2 according to the absence ($\alpha = 1$) or the occurrence ($\alpha > 1$) of the enantioseparation, respectively. Since both Jurs and Shadow descriptors strongly depend on the configurational and conformational aspects of the analyte, their appraisal was carried out using the global minimum conformer as calculated for both the (R)- and (S)-isomers of all the compounds. Thus, two different classification models were built using the (R)- and (S)-enantiomers groups (Tables 4 and 5).

The specific physico-chemical features of the employed chiral selector have resulted decisive in establishing which property of the analyte is responsible for the enantioselectivity accomplishment. Accordingly, for both enantiomers the partial positive surface area (PPSA-1) has been found to be the suitable descriptor for ratio-

Table 4

Partition tree of the (R)-enantiomers of the training set with (R)-SDC

Class	Group	Compounds	Population%	Class% observed corrected	Overall% predicted corrected	Enrichment
1 ($\alpha = 1$)	1	11	34.38	72.73	100.00	2.91
2 ($\alpha > 1$)	2	21	65.62	100.00	87.50	1.33

Table 5Partition tree of the (*S*)-enantiomers of the training set with (*R*)-SDC

Class	Group	Compounds	Population%	Class% observed corrected	Overall% predicted corrected	Enrichment
1 ($\alpha = 1$)	1	11	34.38	63.64	100.00	2.51
2 ($\alpha > 1$)	2	21	65.62	100.00	84.00	1.28

nalizing the observed chromatographic behaviour when the most lipophilic and aromatic (*R*)-STC was adopted [33]. This descriptor is relative to the sum of the solvent-accessible surface areas of all the partially charged atoms. Thus, the model underlines the pivotal role of the π /cation interaction between this area on each analyte and the aromatic portion of the discriminating agent. Interestingly, two descriptors have been identified for understanding the responses achieved with (*R*)-SBC [33]. Indeed, depending on the isomer of the training set used, two different descriptors were selected as splitting nodes of the relative partition tree. Thus, while the fractional negatively charged partial surface area (ratio between the sum of the product of solvent-accessible surface area and partial charge for all negatively charged atoms, and the total molecular solvent-accessible surface area, FNSA-3) was identified as the discriminating descriptor for the (*R*)-enantiomers of the training set, the relative polar surface area (the total polar surface area divided by the total molecular solvent-accessible surface area, RPSA) was selected as the splitting node of the (*S*)-enantiomers. With this selector, polar interactions seem to be responsible for its discriminating activity, probably due to the contribution of the hydrogen bond acceptor ability of the sulfur atom and/or the hydrogen bond donor/acceptor property of free silanols.

It has turned out that the total hydrophobic surface area (TASA) is the suitable descriptor for explaining the observed chromatographic behaviour when the selector endowed with the intermediate lipophilicity [(*R*)-SDC] is employed. This descriptor entails for the sum of the solvent-accessible surface areas of atoms with absolute values of partial charge less than 0.2. Thus, as rule of thumb, (*R*)- and (*S*)-enantiomers characterized by $TASA > 133.8 \text{ \AA}^2$ and 121.9 \AA^2 , respectively, experience separation (Fig. 4). While 73% of correct classification has been observed for class 1 when the study was performed on the set of (*R*)-enantiomers, the correctness of prediction underwent a reduction to 64% for (*S*)-ones. This is ascribed to citrulline (Cit) which although correctly classified in the model of (*R*)-enantiomers, behaves as a false positive in that built with their antipodes. Conversely, for both partition trees, 100% of correct classification has been revealed for class 2. The selection of TASA as the splitting node of this partition tree can be interpreted on the basis of the influence exerted by the interaction between the hydrophobic, wide electron rich aromatic system of (*R*)-SDC and the total hydrophobic surface area of the analyte in stabilizing the diastereomeric complexes in the stationary phase and, consequently, in determining a separating or *non*-separating behaviour of a definite enantiomer couple.

The combination of the two models separately obtained for (*R*)- and (*S*)-enantiomers has allowed to slightly improve the number of corrected classifications. Indeed, while Cit was wrongly classified in the partition tree of (*S*)-enantiomers as a member of class 2, it assumed a borderline behaviour in the combined partition tree of the two individual models (Fig. 5). It is to be mentioned that the two analytes Orn and F94C behave as two false positives, in that they are wrongly classified as belonging to class 2. Ornithine, which represents one of the two basic amino acids used in this study, displays a separating behaviour which is in contrast to the one observed for Arg that, conversely, does separate ($\alpha = 2.29$). As previously stated, when the (*R*)-STC and (*R*)-SBC were employed as the chiral selectors [26], the lack of accuracy of the partition tree in correctly classifying Orn was ascribed to the different aminic

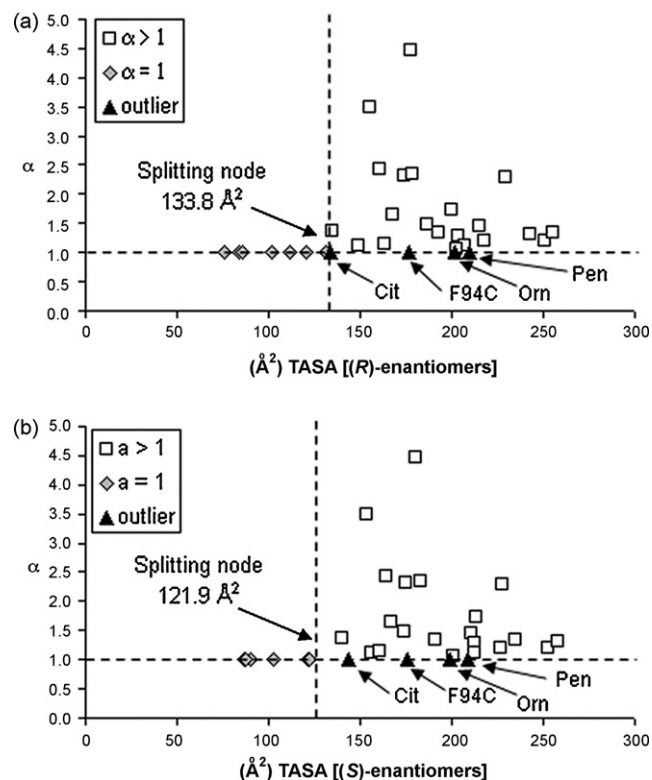


Fig. 4. Plot of α vs. TASA values for (a) (*R*)-enantiomers and (b) (*S*)-enantiomers with the (*R*)-SDC as the chiral selector. The plot shows that (*R*)- and (*S*)-enantiomers endowed with $TASA > 133.8 \text{ \AA}^2$ and 121.9 \AA^2 , generally have α values > 1 with some exceptions (see text for details). Experimental conditions: mobile phase, 1.0 mM Cu(II) sulphate; flow rate, 1.0 mL/min; injection volume, 20 μ L; UV at 254 nm; column temperature, 20 °C.

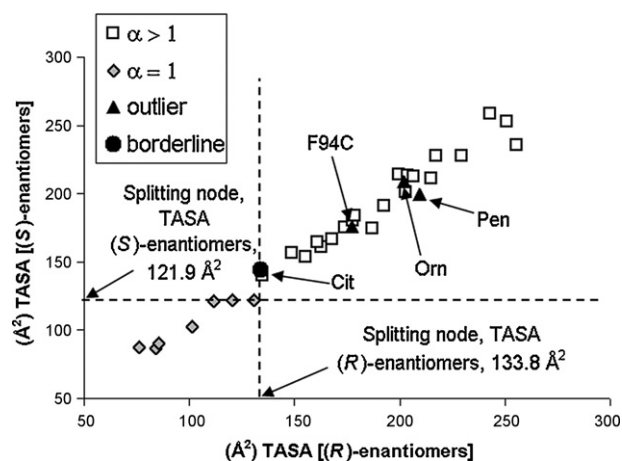
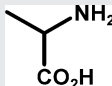
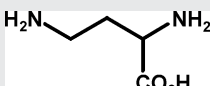
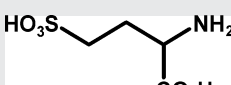
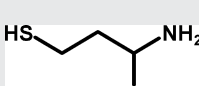
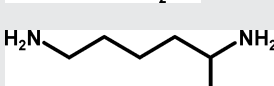
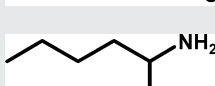
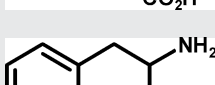
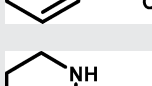


Fig. 5. Combined separation model with (*R*)-SDC as the chiral selector. The plot shows that the exceptions observed in Fig. 4 are less when the two statistical models of DSSR are combined. Experimental conditions: mobile phase, 1.0 mM Cu(II) sulphate; flow rate, 1.0 mL/min; injection volume, 20 μ L; UV at 254 nm; column temperature, 20 °C.

Table 6
Structures and selected chromatographic parameters for the validation-set investigated in this study

Sample	Structure	(R)-STC			(R)-SDC			(R)-SBC		
		k_R	k_S	α	k_R	k_S	α	k_R	k_S	α
Ala		0.73	0.73	1.00	0.45	0.45	1.00	0.92	0.92	1.00
DABA		0.46	0.46	1.00	0.28	0.28	1.00	0.82	0.82	1.00
Homo-CA		0.89	0.89	1.00	0.01	0.01	1.00	0.72	0.72	1.00
Homo-Cys		14.91	26.49	1.78	55.80	67.22	1.20	17.00	62.67	3.69
Lys		0.88	0.88	1.00	0.64	0.64	1.00	0.98	0.98	1.00
Nor-Leu		13.54	21.73	1.61	17.35	22.88	1.32	18.27	27.90	1.53
Phe		44.94	79.39	1.66	66.06	68.60	1.04	81.41	148.26	1.82
Pip		4.55	29.39	6.45	4.20	5.26	1.25	9.47	38.56	4.07

Experimental conditions: mobile phase, 1.0 mM Cu(II) sulphate; flow rate, 1.0 mL/min; injection volume, 20 μ L; UV at 254 nm; column temperature, 20 °C.

functionality of the side chain. Thus, while the tiny primary amine group of (R)- and (S)-Orn may interact with the central copper ion of the chiral complex through coordinative bonds, the planar and large guanidine moiety of Arg is too cumbersome to promote such interactions. Thus, the additional interaction of Orn, regardless to the (S)- or (R)-enantiomer, may catch the analyte side chain from interacting with the aromatic system of the chiral selector, hence hampering the enantiodiscrimination. Similarly, the heterocyclic ring of the isomer F94C may also be involved in interactions with the central copper ion that affect the separation behaviour of the analyte. Once again, also penicillamine (Pen) behaves as a false positive being wrongly assigned to class 2. The erroneous classification can be plausibly deputed to its well known tri-dentate behaviour when coupled with copper(II) cations.

In order to validate and test the predictive power of our partition trees, also with (R)-SDC, the separating behaviour of an external test set of eight aminoacidic compounds was assessed (Table 6). The experimental results were compared with the class membership proposed by the classification models. The inspection of the observed and predicted class membership of the validation set reveals that six out of eight analytes are correctly inserted in class 2 (five compounds) and class 1 (one compound). Interestingly, the basic amino acids lysine (Lys) and diaminobutyric acid (DABA) are false positives in both models. Since the side chains of these analytes carry a primary amine group, this observation sustains the

hypothesis that the proposed classification models neglect specific interaction features of the analyte that affect its separating behaviour. As discussed above, one of these features is the presence of a primary amine group in the side chain of the analyte that may interact with the central copper ion of the chiral complex through an additional coordinative bond.

4. Conclusion

In this work, we have confirmed an our previous finding that the (R)-STC selector almost always provides for the best performance in terms of enantioseparation ability. Moreover, although the heterogeneity accompanying each chiral-coated phase renders difficult classical mechanistic investigations, innovative classification studies have been successfully engaged. Accordingly, as a continuation of our work in the field of descriptive structure–separation relationship study, we have investigated the development of a classification model to qualitatively explain the separation behaviour of 32 enantiomeric mixtures of amino acids using S-diphenylmethyl-(R)-cysteine as the chiral selector. In particular, using a partition tree analysis and a pool of molecular shape and electrotopological descriptors, we have provided a classification model that sheds new light on the molecular features affecting the separation of enantiomer couples of amino acids in the chromatographic process of CLEC. While PPSA seems to be the most

influencing descriptor with (*R*)-STC, TASA plays a governing role with (*R*)-SDC. With (*R*)-SBC as the chiral selector, (*R*)- and (*S*)-enantiomers differ in the controlling electrotopological descriptor: while (*R*)-enantiomers feel the effect of FNSA-3, (*S*)-enantiomers are best discriminated by the information encoded in RPSA-1. The results are found in good agreement with the previously reported descriptive structure–separation relationship of amino acids with (*R*)-STC and (*R*)-SBC. Furthermore, the good predictivity shown by the classification model will be fruitful to select amino acids to be separated with (*R*)-SDC on a preparative scale. Further molecular modelling studies as well as a crystallographic analysis are underway and will be reported in due course.

References

- [1] K. Klak, A. Palucha, P. Brański, M. Sowa, A. Pilc, *Amino Acids* 32 (2007) 169.
- [2] M. Pietraszek, J. Nagel, A. Gravius, D. Schäfer, W. Danysz, *Amino Acids* 32 (2007) 173.
- [3] P. Bonsi, D. Cuomo, B. Picconi, G. Sciamanna, A. Tschertter, M. Tolu, G. Bernardi, P. Calabresi, A. Pisani, *Amino Acids* 32 (2007) 189.
- [4] K. Ossowska, J. Konieczny, J. Wardas, M. Pietraszek, K. Kuter, S. Wolfarth, A. Pilc, *Amino Acids* 32 (2007) 179.
- [5] W. Wu, D.A. Burnett, M. Domalski, W.J. Greenlee, C. Li, R. Bertorelli, S. Fredduzzi, G. Lozza, A. Veltri, A. Reggiani, *J. Med. Chem.* 50 (2007) 5550.
- [6] G. Mannaioni, M. Alesiani, V. Carla, B. Natalini, M. Marinozzi, R. Pellicciari, F. Moroni, *Eur. J. Pharmacol.* 251 (1994) 20.
- [7] R. Pellicciari, R. Luneia, G. Costantino, M. Marinozzi, B. Natalini, P. Jakobsen, A. Kanstrup, G. Lombardi, F. Moroni, C. Thomsen, *J. Med. Chem.* 38 (1995) 3717.
- [8] R. Pellicciari, M. Marinozzi, B. Natalini, G. Costantino, R. Luneia, G. Giorgi, F. Moroni, C. Thomsen, *J. Med. Chem.* 39 (1996) 2259.
- [9] G. Costantino, A. Macchiarulo, R. Pellicciari, *J. Med. Chem.* 42 (1999) 2816.
- [10] G. Costantino, M. Marinozzi, E. Camaioni, B. Natalini, I. Sarichelou, F. Micheli, P. Cavanni, S. Faedo, C. Noe, F. Moroni, R. Pellicciari, *Il Farmaco* 59 (2004) 93.
- [11] R. Pellicciari, R. Filosa, M.C. Fulco, M. Marinozzi, A. Macchiarulo, C. Novak, B. Natalini, M.B. Hermit, S.M. Nielsen, T.N. Sager, T.B. Stensboel, C. Thomsen, *ChemMedChem* 1 (2006) 358.
- [12] L. Amori, M. Serpi, M. Marinozzi, G. Costantino, M. Gavilan Diaz, M.B. Hermit, C. Thomsen, R. Pellicciari, *Bioorg. Med. Chem. Lett.* 16 (2006) 196.
- [13] R. Pellicciari, M. Marinozzi, A. Macchiarulo, M.C. Fulco, J. Gafarova, M. Serpi, G. Giorgi, S. Nielsen, C. Thomsen, *J. Med. Chem.* 50 (2007) 4630.
- [14] B. Natalini, M. Marinozzi, K. Bade, R. Sardella, C. Thomsen, R. Pellicciari, *Chirality* 16 (5) (2004) 314.
- [15] B. Natalini, R. Sardella, A. Macchiarulo, R. Pellicciari, *J. Sep. Sci.* 31 (2008) 696.
- [16] B. Natalini, R. Sardella, A. Macchiarulo, A. Massarotti, R. Pellicciari, *J. Sep. Sci.*, in press.
- [17] D.T. Stanton, P.C. Jurs, *Anal. Chem.* 62 (1990) 2323.
- [18] R.H. Roxburgh, P.C. Jurs, *Anal. Chim. Acta* 199 (1987) 99.
- [19] M.H. Abraham, *Anal. Chem.* 69 (1997) 613.
- [20] T. Suzuki, S. Timofei, B.E. Iouras, G. Uray, P. Verdino, W.M.F. Fabian, *J. Chromatogr. A* 922 (2001) 13.
- [21] C.A. Montanari, Q.B. Cass, M.E. Tiritan, A.L.S. de Souza, *Anal. Chim. Acta* 419 (2000) 93.
- [22] V. Andrisano, T.D. Booth, V. Cavrini, I.W. Wainer, *J. Chromatogr. A* 876 (2000) 75.
- [23] M. Lämmerhofer, P. Franco, W. Lindner, *J. Sep. Sci.* 29 (2006) 1486.
- [24] W.M.F. Fabian, W. Stampfer, M. Mazur, G. Uray, *Chirality* 15 (2003) 271.
- [25] F. Moroni, S. Attucci, A. Cozzi, E. Meli, R. Picca, M.A. Schkeider, R. Pellicciari, C. Noe, I. Sarichelou, D.E. Pellegrini-Giampietro, *Neuropharmacology* 42 (2002) 741.
- [26] P. Conti, M. De Amici, G. De Sarro, M. Rizzo, T.B. Stensbøl, H. Bräuner-Osborne, U. Madsen, L. Toma, C. De Micheli, *J. Med. Chem.* 42 (1999) 4099.
- [27] H.Y. Aboul-Enein, M.I. El-Awady, C.M. Heard, *Biomed. Chromatogr.* 17 (2003) 325.
- [28] M. Kele, G. Guiochon, *J. Chromatogr. A* 960 (2002) 19.
- [29] V.A. Davankov, *Chirality* 9 (1996) 99.
- [30] V.A. Davankov, A.S. Bochkov, A.A. Kurganov, P. Roumeliotis, K.K. Unger, *Chromatographia* 13 (1980) 677.
- [31] G. Götmar, T. Fornstedt, G.G. Guiochon, *Chirality* 12 (2000) 558.
- [32] Z. Chilmoneczyk, H. Ksycińska, M. Lisowaka-Kuźmich, A. Jofczyk, M. Mazgajska, M. Jarończyk, A. Strzelczyk, H.Y. Aboul-Enein, *Anal. Chim. Acta* 536 (2005) 7.
- [33] T. Fornstedt, P. Sajonz, G. Guiochon, *J. Am. Chem. Soc.* 119 (1997) 1254.
- [34] W.R. Oberleitner, N.M. Maier, W. Lindner, *J. Chromatogr. A* 960 (2002) 97.
- [35] V.A. Davankov, *J. Chromatogr. A* 666 (1994) 55.
- [36] V.A. Davankov, in: D. Cagniant (Ed.), *Complexation Chromatography*, Marcel Dekker, New York, 1992, p. 197.
- [37] B. Natalini, R. Sardella, A. Macchiarulo, R. Pellicciari, *Chirality* 18 (2006) 509.